3E8. ZKP WING, OSCILLATING AILERON

by
Dipi. Ing. K.Dau
Dipi. Ing. S.Vogel
Dipi. Ing. H.Zimmermann
MBB Transport und Verkehrsflugzeuge
TE234
Postfach 10 78 45
2800 Bremen 1
Germany

INTRODUCTION

This Data Set contains pressure distributions measured on the ZKP wing for an oscillating aileron in the ONERA transonic 51 wind tunnel at Modane, France, in late 1982. The tests were part of a cooperative project between MBB, ONERA, and the Aerospatiale Corporation. The purpose of the tests was to obtain steady and unsteady pressures due to fast-moving control surfaces in transonic flow, likely to be encountered in the operation of active control systems for transport aircraft.

The following is a number of comments on the diagrams and tables.

GEOMETRY OF EXPERIMENTAL MODEL

The model geometry is shown in Fig. 3 to 5. Figure 3 shows the model including the major dimensions of the half-fuselage in a coordinate system parallel to the tunnel floor and walls. Figure 4 shows the dimensions of the wing and the aileron when rotated by the dihedral angle of 4.787 deg into the plane z = 0 of the coordinate system in which the profile coordinates are given by Ref. 1. Figure 5 shows the details of the aileron geometry in cross-section, including nose and gap geometry.

COMPARISON WITH AGARD COMPUTATIONAL PROGRAMME OF REF. 1

Model geometry

Unlike the computational model (Ref. 1, Fig. 7) the experimental model has a half-fuselage as shown in Fig. 3. This changes the definition of the root chord which is now smaller than the computational root chord because of the taper of the wing (see Fig. 4). The difference in the definition of the root chord affects the specifications of reduced frequency and Reynolds number as shown in Para. 12, NOTATION. Otherwise the two planforms and their coordinate origins are identical. Furthermore, the gap between aileron and wing spar (Fig. 5) of the experimental model was not sealed, as stated in Ref. 1. The gap is 0.3-0.5 mm wide.

Instrumentation

The number and location of the sections at which pressures were measured where changed from the values given in Ref. 1 to those given in Fig. 6.

Design Condition

The design condition of the experimental model is M = 0.78 and $\alpha_m = 1.5^o$ as listed in Ref. 1, Sect. 3.4. The experimental lift coefficient may be somewhat different from the listed theoretical value of 0.5 at the design condition, depending on how the fuselage contribution is interpreted.

Experimental Cases

The experimental cases for which data are provided in the Data Set are not identical with the computational test cases originally suggested in Ref.1, Table 9; this may affect the choices for future calculations. The correspondence between the experimental and the original computational cases is shown in Table 2. It will be seen that, of the computational choices, only the three priority cases have closely related experimental cases. No experimental results are available for M = 0.73 to match the computational cases 2 and 3.

TEST SET-UP AND INSTRUMENTATION

The wind tunnel test set-up for measuring unsteady pressures on the wing is shown in Fig.1 and 2. To prevent the wing tip from executing large bending motions due to aileron forces, the wing tip was braced by four cables, all attached to a point of the wing tip, and lying in a plane roughly parallel to the aircraft plane of symmetry. The other ends of the cables were led outside the test section, and preloaded with a two-ton weight each.

Prior to every unsteady run the brakes on all cables were released permitting the wing to assume mean position under aerodynamic load without additional cable constraint, while the new mean test parameters (Mach no., wing and flap incidences) were established. The cables were then clamped, and remained clamped during aileron oscillation.

The aileron was actuated by a hydraulic servo motor producing a harmonic aileron rotation about ts swept hinge axis. The instantaneous aileron displacement was measured relative to the wing by potentiometers in the streamwise direction at the two aileron stations.

The wing was equipped with 509 pressure taps for steady pressures, and 387 Kulite transducers for unsteady pressures. The tap coordinates are listed in Tables 3 to 7 with their corresponding pressures.

The pressure taps were arrayed in streamwise wing sections as shown in Fig.6. For reasons of space the sections containing steady-pressure taps were not congruent with those for unsteady pressures, but are considered to be close enough to reflect flow conditions for the neighboring unsteady pressures with sufficient accuracy for most purposes.

Steady pressures were measured via tubing and scanivalve by tunnel system transducers, unsteady pressures were measured by Kulite transducers installed directly below each pressure tap. Furthermore 17 accelerometers were installed on the wing, one of them on the aileron, see Fig.7.

DATA PROCESSING

Only the fundamental component was recorded for each response signal . Response signal phase was defined to be relative to aileron motion. All listed pressures correspond to an aileron amplitude of δ_0=1°, the aileron deflection angles δ_m, and δ_0 being defined in the streamwise direction.

Both steady and unsteady pressures are presented in uncorrected form. Those pressure values which were obviously spurious (transducer failure, etc.) were eliminated. Besides these data additional data, listed in Table 1, could be made available.

DISCUSSION

The unsteady pressures generally exhibit the distribution typical for ailerons on transport aircraft wings, i.e. they are virtually zero outside the neighborhood of the aileron sections. Therefore only the aileron section pressures are shown as plots against x/c on Fig.8 to 14.

Concerning the sectional lift and moment coefficients, which are listed in the same tables as the pressure distribution from which they were derived, it should be pointed out that they are uncorrected in the sense that no attempt has been made to introduce supplementary points where a pressure peak was obviously not properly defined by the array of pressure taps, see for instance Fig.11, top left plot. Furthermore the integration interval extended only from the first to the last tap on a given section. The section coefficients should therefore be viewed only as a rough guide to the spanwise distribution.

Because of the uncorrected values, the spanwise distribution of load coefficients is likely to show some fluctuation. The wiggle near the wing tip, however, seems to be genuine; and is believed to have been caused by a geometric irregularity behind the aileron gap.

During the course of the test program certain steady test cases were repeated a number of times for nominally the same test parameters. Since repeatability is a good indicator of data quality, the pressures on the mid-aileron section have been plotted on top of each other for a number of nominally identical cases, see Fig.15.

The right-hand plot corresponds to five runs, one of which (case 94) was made entirely without wing-tip cable braces, entailing a tunnel shut-down before the remaining cases were run. In spite of the shut-down, repeatability may be said to be very good. The left-hand plot shows pressures for a larger number of repetitions for the same case, with two intervening shut-downs. Agreement here is still good, but two runs show a marked deviation from the mean near the hinge position, which is known to be sensitive to changes in flow parameters. The two runs in question were separated by two shut-downs from the other runs of the series.

No comparable repetitions were made for unsteady pressures, but they are felt to be of the same quality as the steady ones.

LIST OF SYMBOLS AND DEFINITIONS

ALPHA	α_m	mean wing incidence, as defined in 5.9
C	c	local chord
CL	c_l	sectional lift coefficient
CM	c_m	sectional moment coefficient about quarter-chord point
CPL	C_p	lower surface
CPU	C_p	upper surface
CPL/RAD		lower surface) unsteady pressure coefficients
CPU/RAD		uppersurface) per unit amplitude
DELM	δ_m	mean streamwise aileron angle
	δ_0	streamwise aileron angle amplitude of oscillation
FREQ	f	frequency
K		reduced frequency based on half-chord at wing-body junction, AGARD k = 1.197k
PTOT	p	total pressure
QINF	q	dynamic pressure

RE		Reynolds number, based on chord at wing-body junction, AGARD Re = 1.197 Re
S	s	semi-span
T0	T_o	total temperature of flow
X/C		non-dimensional chordwise position aft of local leading edge
Y/S	η	spanwise position relative to plane of symmetry

PRESENTATION OF DATA

The data which were presented in tables 3 to 7 of Report 702 for this test are supplied here as a single ASCII data file SET8.UND in RUNAD format as defined in the introduction to chapter 3. The table numbers are used as the "run numbers" for data selection by the program RUNAD. Also supplied as an ASCII file SET8.TAB containing the data formatted into tables.

FORMULARY

General Description of model

1.1	Designation	ZKP Wing
1.2	Type	Half-model of wing fuselage combination, transport aircraft with oscillating aileron, no tail surfaces
1.3	Derivation	Research wing, representative of a medium-range transport aircraft with a supercritical wing
1.4	Additional remarks	None
1.5	References	None

Model Geometry

2.1	Planform	high aspect ratio, tapered
2.2	Aspect ratio	9
2.3	Leading edge sweep	30.08°
2.4	Trailing edge sweep	20.89° for outer wing
2.5	Taper ratio	0.26
2.6	Twist	washout type, see ref. 1, table 4
2.7	Root chord	1.5055m
2.8	Semi-span of model	4.0161m
2.9	Area of planform	3.5989m^2
2.10	Location of reference sections and definition of profiles	15%, 40%, and 85% semi-span (see ref.1 section 2.4)
2.11	Lofting procedure between reference sections	Linear on constnat-chord lines between reference sections (ss ref.1, section 2.4)
2.12	Form of wing-body junction	Gap between half-fuselage and floor sealed with brushes
2.13	Form of wing tip	rounded
2.14	Control surface details	unsealed aileron-wing gap about 0.3 to 0.5 mm wide (see fig.5)
2.15	Additional remarks	None
2.16	References	None

Wind Tunnel

3.1	Designation	ONERA S1 transonic tunnel, Modane, France
3.2	Type of tunnel	Closed circuit, ambient pressure
3.3	Test section dimensions	6.855m high and wide, 14.0m long (see fig.1 and 2)
3.4	Type of roof and floor	Solid, excpet for 2 slots (see also fig.1 and 2)
3.5	Type of side walls	Solid

3.6	Ventilation geometry	One slot each at intersection of floor with wind tunnel shell, 0.13m wide, running from 5m to 9m from test section entrance
3.7	Thickness of side wall boundary layer	about 0.1m
3.8	Thickness of boundary layers at roof and floor	about 0.1m
3.9	Method of measuring Mach number	by measurement of static pressure, 4.5m upstream of test section, and by previous calibration
3.10	Flow angularity	Not measured
3.11	Uniformity of velocity over test section	Not measured
3.12	Sources and levels of noise or turbulence in empty tunnel	Considered very small
3.13	Tunnel resonances	At f = N/5, N/6, N/5 + N/6, N=246 M
3.14	Additional remarks	None
3.15	References on tunnel	None

Model motion

4.1	General description	Aileron oscillation with braced wing tip. Amplitude 1 ° and 2°, frequency 6, 12, 21 Hz.
4.2	Natural frequencies and normal modes of model and support system	15.6, 27.3, 44.4 Hz with cable braces

Test Conditions

5.1	Model planform area/tunnel area	0.08
5.2	Model span/tunnel width	0.5858
5.3	Blockage	NA
5.4	Position of model in tunnel	x-mac 6.19m downstream of test section inlet (see fig.1)
5.5	Range of Mach number	0.5, 0.78, 0.83
5.6	Range of tunnel total pressure	0.9 bar
5.7	Range of tunnel total temperature	298 to 322° K
5.8	Range of model steady or mean incidence	-1 to +3°
5.9	Definition of model incidence	The model incidence α_m is defined to be zero when the fuselage reference line (FRL) is parallel to the tunnel walls. The FRL lies in the plane z=0 of the profile coordinate system as listed in ref.1.
5.10	Position of transition, if free	No
5.11	Position and type of trip, if transition fixed	x/c=0.07, upper and lower wing surface, 5mm wide band of 80K carborundum. Same type of trip on fuselage, 105mm from nose.
5.12	Flow instabilities during tests	None detected
5.13	Changes to mean shape of model due to steady aerodynamic load	Not measured
5.14	Additional remarks	None
5.15	References describing tests	None

Measurements and Observations

6.1	Steady pressures for the mean conditions	Y
6.2	Steady pressures for small changes from the mean conditions	Y
6.3	Quasi-steady pressures	6 Hz
6.4	Unsteady pressures	Y
6.5	Steady section forces for the mean conditions by integration of pressures	Y
6.6	Steady section forces for small changes from	N

	the mean conditions by integration	
6.7	Quasi-steady section forces by integration	6 Hz
6.8	Unsteady section forces by integration	Y
6.9	Measurement of actual motion at points of model	Y
6.10	Observation or measurement of boundary layer properties	N
6.11	Visualisation of surface flow	N
6.12	Visualisation of shock wave movements	N
6.13	Aditional remarks	None

Instrumentation

7.1	Steady pressure	
	7.1.1 Position of orifices spanwise and chordwise	See fig.6 and tables 3 to 7.
	7.1.2 Type of measuring system	Taps connected via tubing and Scanivalve to tunnel system transducers
7.2	Unsteady pressure	
	7.2.1 Position of orifices spanwise and chordwise	See fig.6 and tables 3 to 7.
	7.2.2 Diameter of orifices	0.3mm
	7.2.3 Type of measuring system	Transducer installed directly below each tap.
	7.2.4 Type of transducers	Kulite
	7.2.5 Principle and accuracy of calibration	Calibrated by 30 Hz sinusoidal signal before tests. Checked at various intervals during testing. Variation less than 1%.
7.3	Model motion	
	7.3.1 Method of measuring motion reference coordinate	Aileron angle measured relative to wing structure by rotary potentiometers on aileron. Aileron harmonic rotation about swept axis at the 77.4% chord line, measured at inboard and centre aileron section.
	7.3.2 Method of determining spatial mode of motion	By accelerometers on wing and aileron, and potentiometers on aileron.
	7.3.3 Accuracy of measured motion	2%
7.4	Processing of unsteady measurements	
	7.4.1 Method of acquiring and processing measurements	Signal digitized (12 bit ADC) and Fourier transformed. Transfer function for motion-pressure by HP 5451 Analyzer.
	7.4.2 Type of analysis	Only one harmonic kept.
	7.4.3 Unsteady pressure quantities obtained and accuracies achieved	Presented data are amplitudes of fundamental of all response signals. Response phases are defined relative to zero aileron deflection.
	7.4.4 Method of integration to obtain forces	Cubic spline, uncorrected for possible missed peaks. Integration interval between first and last pressure taps on section.
7.5	Additional remarks	None
7.6	References on techniques	None

Data presentation

8.1	Test cases for which data could be made available	Table 1.
8.2	Test cases for which data are included in this document	Table 2.
8.3	Steady pressures	Tables 3 to 7.
8.4	Quasi-steady or steady perturbation	6 Hz, unsteady pressures

	pressures	
8.5	Unsteady pressures	Tables 3 to 7.
8.6	Steady forces or moments	Tables 3 to 7.
8.7	Quasi-steady or unsteady perturbation forces	6 Hz, unsteady loads
8.8	Unsteady forces and moments	Tables 3 to 7.
8.9	Other forms in which data could be made available	Magnetic tape
8.10	Reference giving other representations of data	2

Comments on data

9.1	Accuracy	
	9.1.1 Mach number	About 0.002
	9.1.2 Steady incidence	About 0.1°
	9.1.3 Reduced frequency	About 2%
	9.1.4 Steady pressure coefficients	See discussion and fig.15
	9.1.5 Steady pressure derivatives	Not calculated
	9.1.6 Unsteady pressure coefficients	See discussion
9.2	Sensitivity to small changes of parameter	Not calculated
9.3	Non-linearities	None detected
9.4	Influence of tunnel total pressure	Total pressure was kept constant
9.5	Effects on data of uncertainty, or variation, in mode of model motion	Not checked
9.6	Wall interference corrections	All pressures are uncorrected
9.7	Other relevant tests on same model	None
9.8	Relevant tests on other models of nominally the same shapes	None
9.9	Any remarks relevant to comparison between experiment and theory	None
9.10	Additional remarks	None
9.11	References on discussion of data	2

Personal contact for further information

Dipl. Phys. H Zimmermann, MBB-Bremen, Abt. TE234 Hunefeldstr. 1-5, 2800 Bremen, Germany

List of references

1 S R Bland. AGARD three-dimensional aeroelastic configurations. AGARD Advisory Report 167, March 1982.

2 M Couston, J J Angelini, J P Meurzec. Compariason des champs de pression instationnaires calcules et mesures sur le modele ZKP. AGARD R-688, April 1980 (Also available as RAE Library translation 2061, November 1980).

Table 1 List of run numbers available

Run parameters						Run indices			
M	p_t (bar)	T_o (°K)	α_m (°)	δ_m (°)	δ_o (°)	Steady	6 Hz	12 Hz	21 Hz
0.50	0.9	297.7	3	-5	1	21	18	-	21
0.50	0.9	297.7	3	0	1	26	23	25 *	26
0.50	0.9	297.7	3	10	1	33	31	-	33
0.78	0.9	311.3	-1	-5	1	58	56	-	58
0.78	0.9	315.9	-1	0	1	75	61	64	75
0.78	0.9	317.4	-1	0	2	144	63	144	-
0.78	0.9	320.8	-1	5	1	80	78	-	80
0.78	0.9	322.6	0	-5	1	90	88	-	90 *
0.78	0.9	322.7	0	0	1	97	94	96	97 *
0.78	0.9	319.2	0	0	2	143	95	143	-
0.78	0.9	322.0	0	5	1	102	-	-	102
0.78	0.9	318.0	2	-5	1	109	107	-	109
0.78	0.9	319.2	2	0	1	116	112	115	116 *
0.78	0.9	316.5	2	0	2	145	114	145	-
0.78	0.9	319.4	2	5	1	119	119	-	121
0.83	0.9	321.6	0	-2	1	141	131	137	140 *
0.83	0.9	321.6	0	0	1	143	133	138	141
0.83	0.9	322.2	0	2	1	145	135	139	142

Note: the starred case numbers correspond to data in tables 3 to 7.

Table 2 Experimental cases for which data are included, related to computational cases of ref 1

Note that amplitude δ_o=1° for all these cases. * indicates priority case

Experimental Case						Computational Case				
Run Index	M	α_m (°)	δ_m (°)	f (Hz)		Case No.	M	α_m (°)	δ_m (°)	f (Hz)
25	0.50	3	0	12		1	0.30	0	-4.60	10
97	0.78	0	0	21		4 *	0.78	0	0	20
90	0.78	0	-5	21		5 *	0.78	0	-5.52	20
116	0.78	2	0	21		6 *	0.78	2	0	20
140	0.83	0	-2	21		7	0.83	0	-5.52	20

Run details for data supplied on electronic media.

Note that table number is used as the reference number in selection program RUNAD.

Table 3	Run index =25	M=0.50	α_m=3°	δ_m =0°	f= 12 Hz
	K=0.336	PTOT=0.900 bar	QINF = 0.133 bar	RE= 0.134E8	T0=297.85 ° K
Table 4	Run index =97	M=0.78	α_m=0°	δ_m =0°	f= 21 Hz
	K=0.375	PTOT=0.900 bar	QINF = 0.255 bar	RE= 0.163E8	T0=322.65 ° K
Table 5	Run index =90	M=0.78	α_m=0°	δ_m =-5°	f= 21 Hz
	K=0.375	PTOT=0.900 bar	QINF = 0.254 bar	RE= 0.163E8	T0=322.55 ° K
Table 6	Run index =116	M=0.78	α_m=2°	δ_m =0°	f= 21 Hz
	K=0.377	PTOT=0.900 bar	QINF = 0.254 bar	RE= 0.165E8	T0=319.15 ° K
Table 7	Run index =140	M=0.83	α_m=0°	δ_m =-2°	f= 21 Hz
	K=0.355	PTOT=0.900 bar	QINF = 0.275 bar	RE= 0.169E8	T0=322.55 ° K

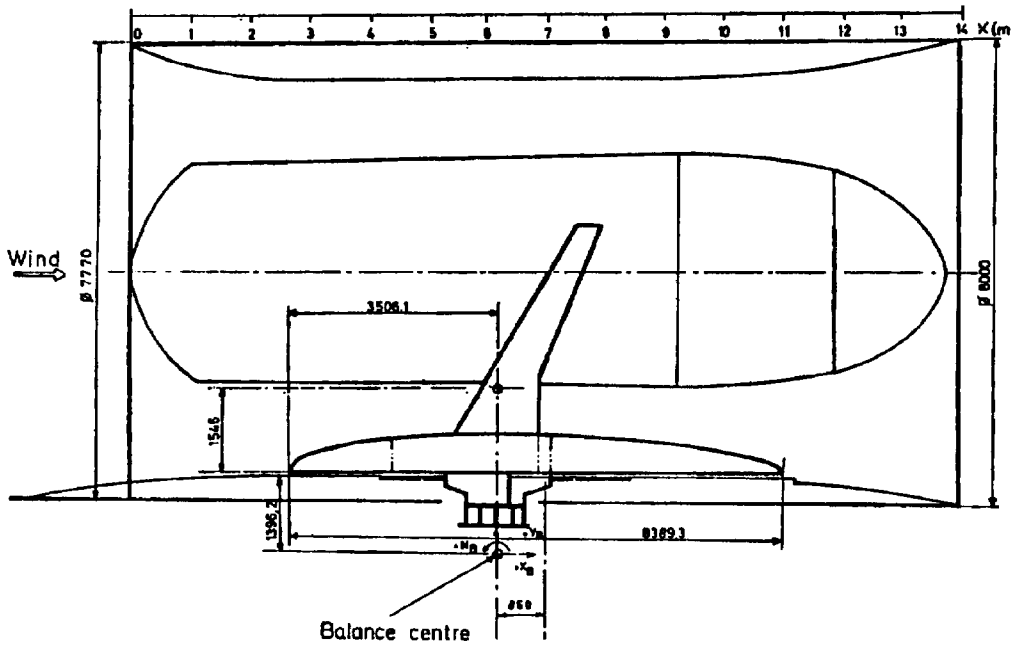

FIG. 1 Model set-up in test section, side view

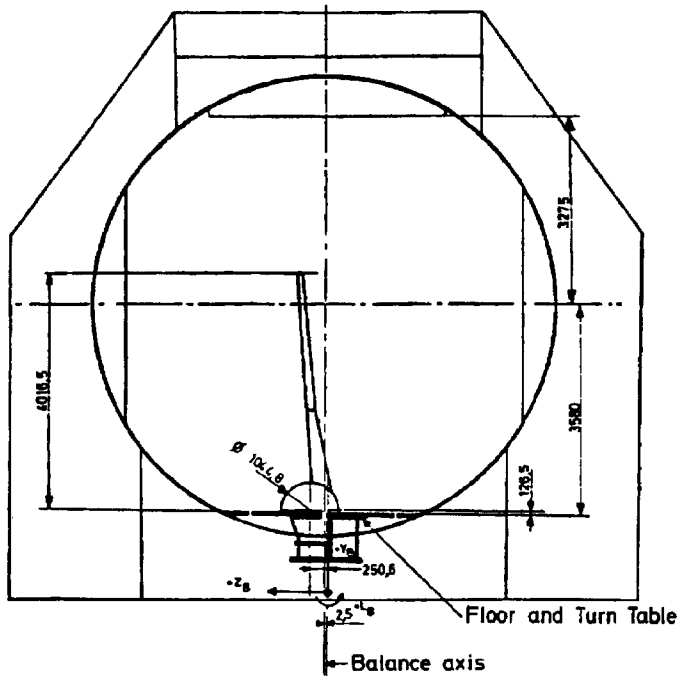

FIG. 2 Model set-up in test section, head-on view

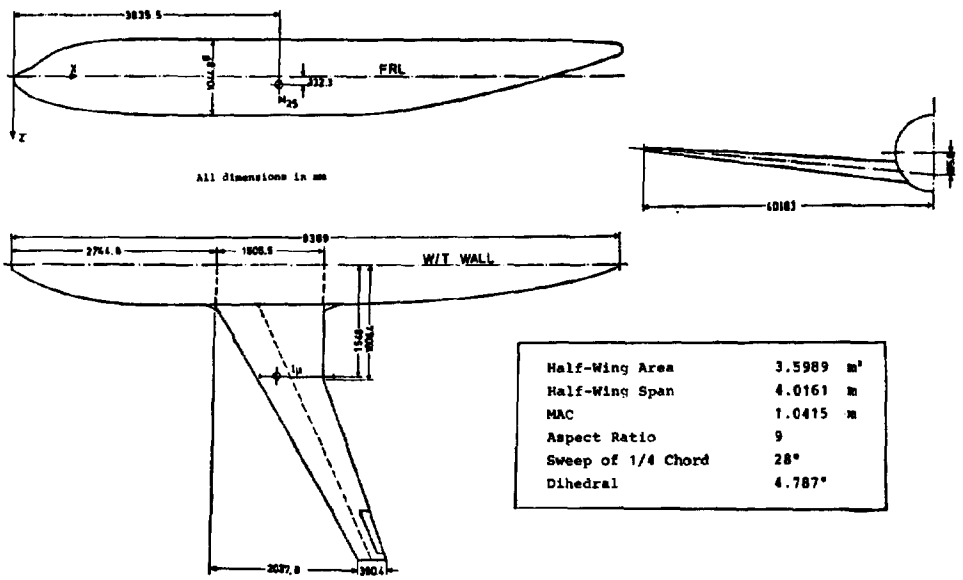

FIG. 3 Geometry of experimental ZKP model

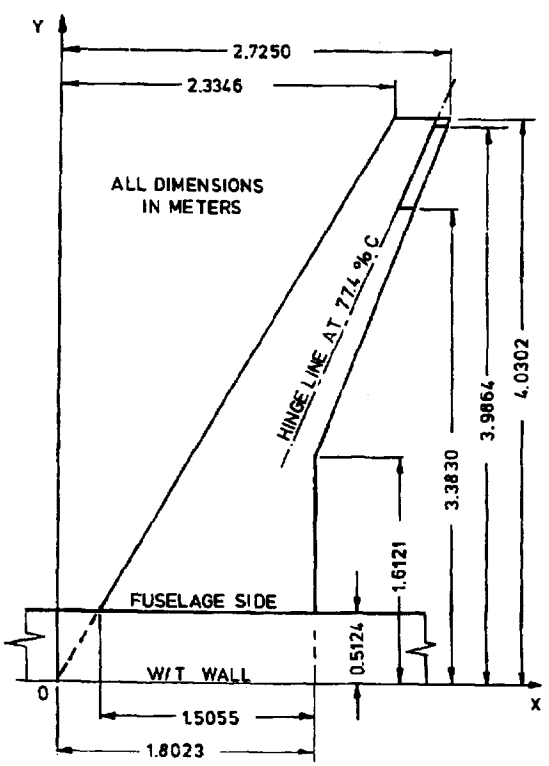

FIG. 4 Geometry of experimental ZKP wing, rotated into profile-coordinate plane by dihedral angle ϕ = 4.787 deg

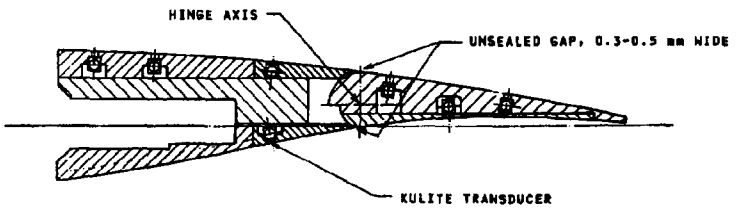

FIG. 5 Aileron geometry in cross-section at wing section 14

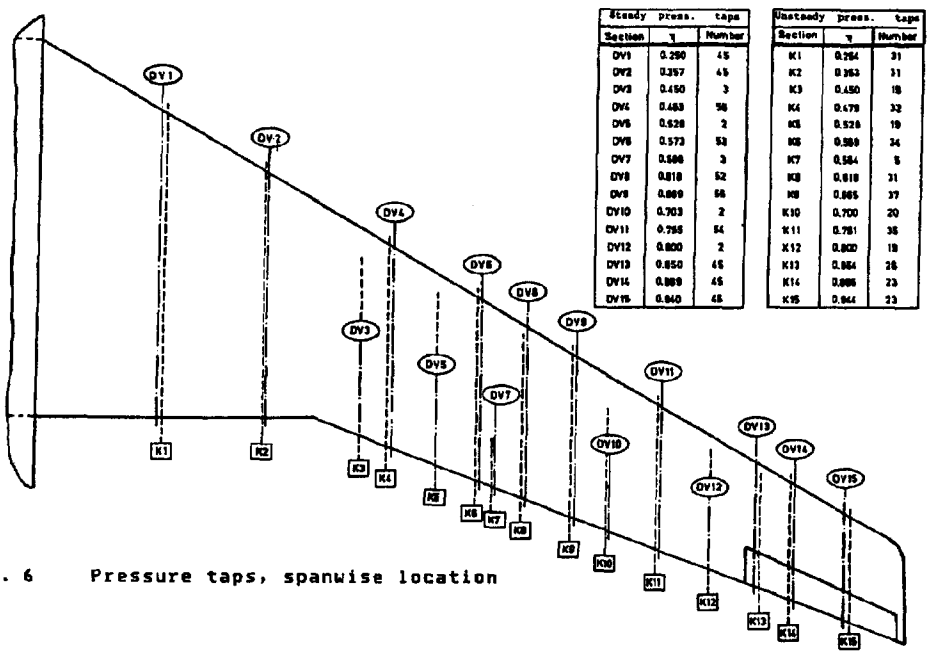

Steady press. taps		
Section	η	Number
DV1	0.290	45
DV2	0.357	45
DV3	0.450	3
DV4	0.483	56
DV5	0.528	2
DV6	0.573	53
DV7	0.606	3
DV8	0.810	52
DV9	0.889	56
DV10	0.703	2
DV11	0.755	54
DV12	0.800	2
DV13	0.850	45
DV14	0.889	45
DV15	0.940	45

Unsteady press. taps		
Section	η	Number
K1	0.284	31
K2	0.353	31
K3	0.450	19
K4	0.479	32
K5	0.526	19
K6	0.589	34
K7	0.584	5
K8	0.810	31
K9	0.885	37
K10	0.700	20
K11	0.751	36
K12	0.800	19
K13	0.864	26
K14	0.886	23
K15	0.944	23

FIG. 6 Pressure taps, spanwise location

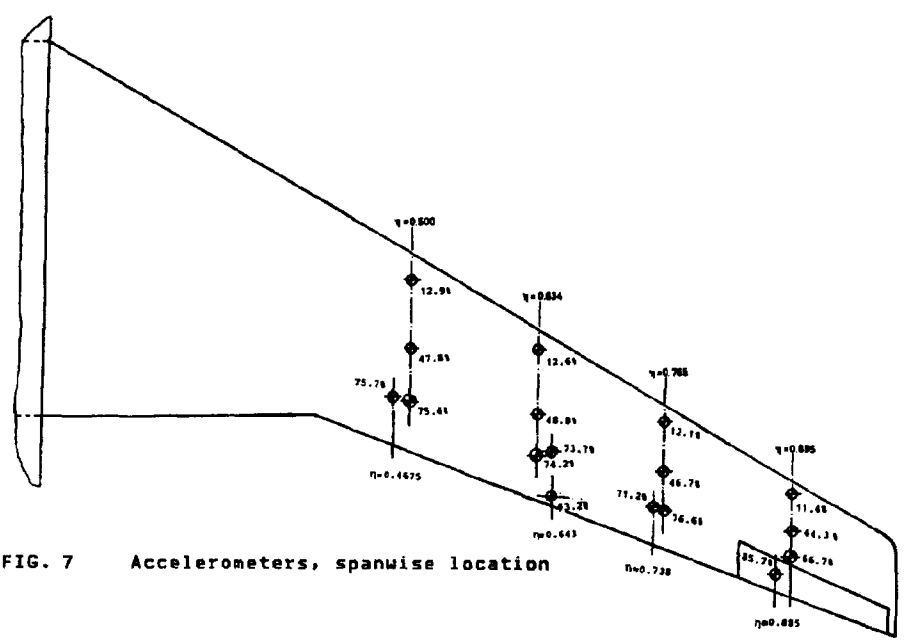

FIG. 7 Accelerometers, spanwise location

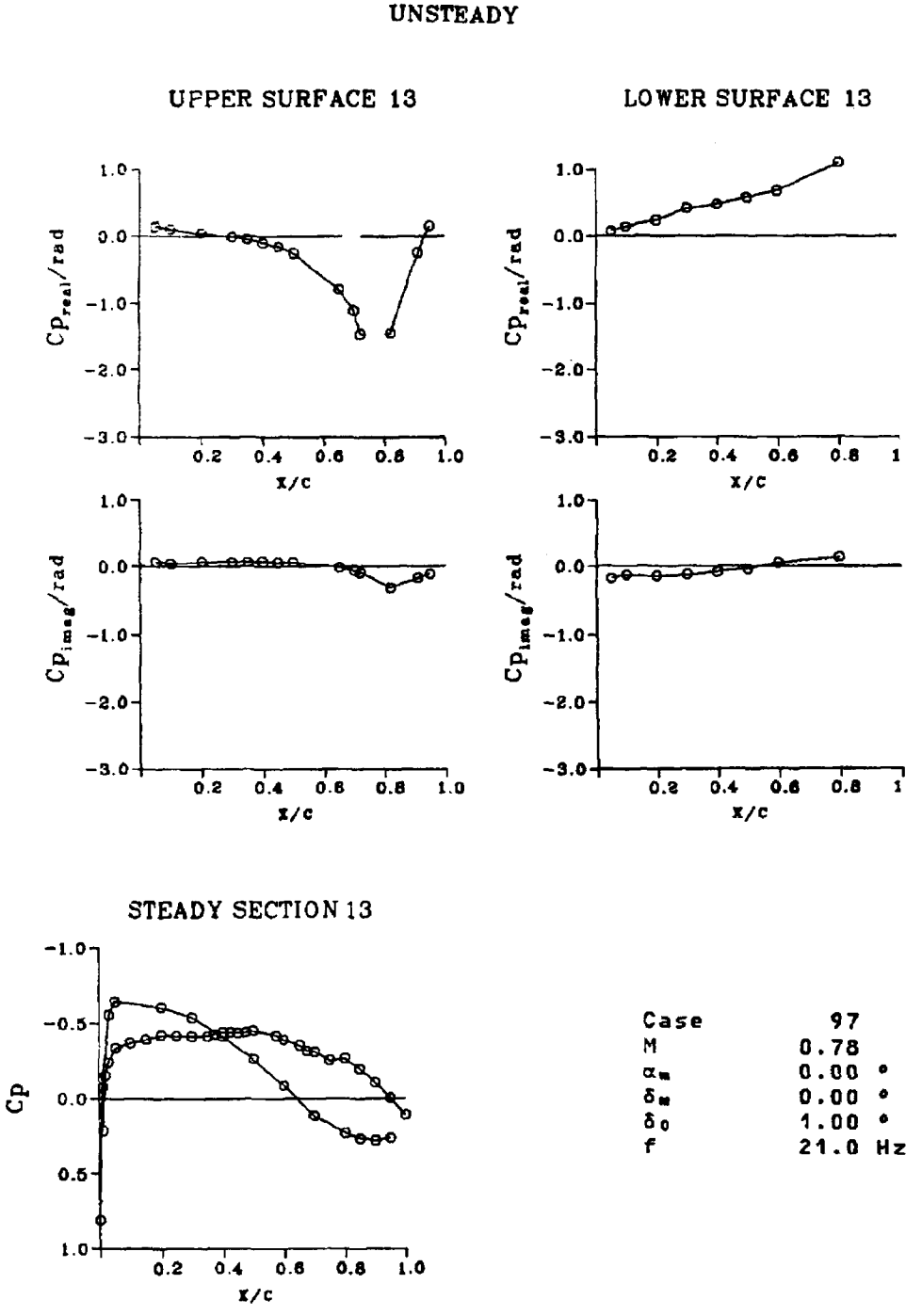

FIG. 8 Sample pressure distribution for aileron section

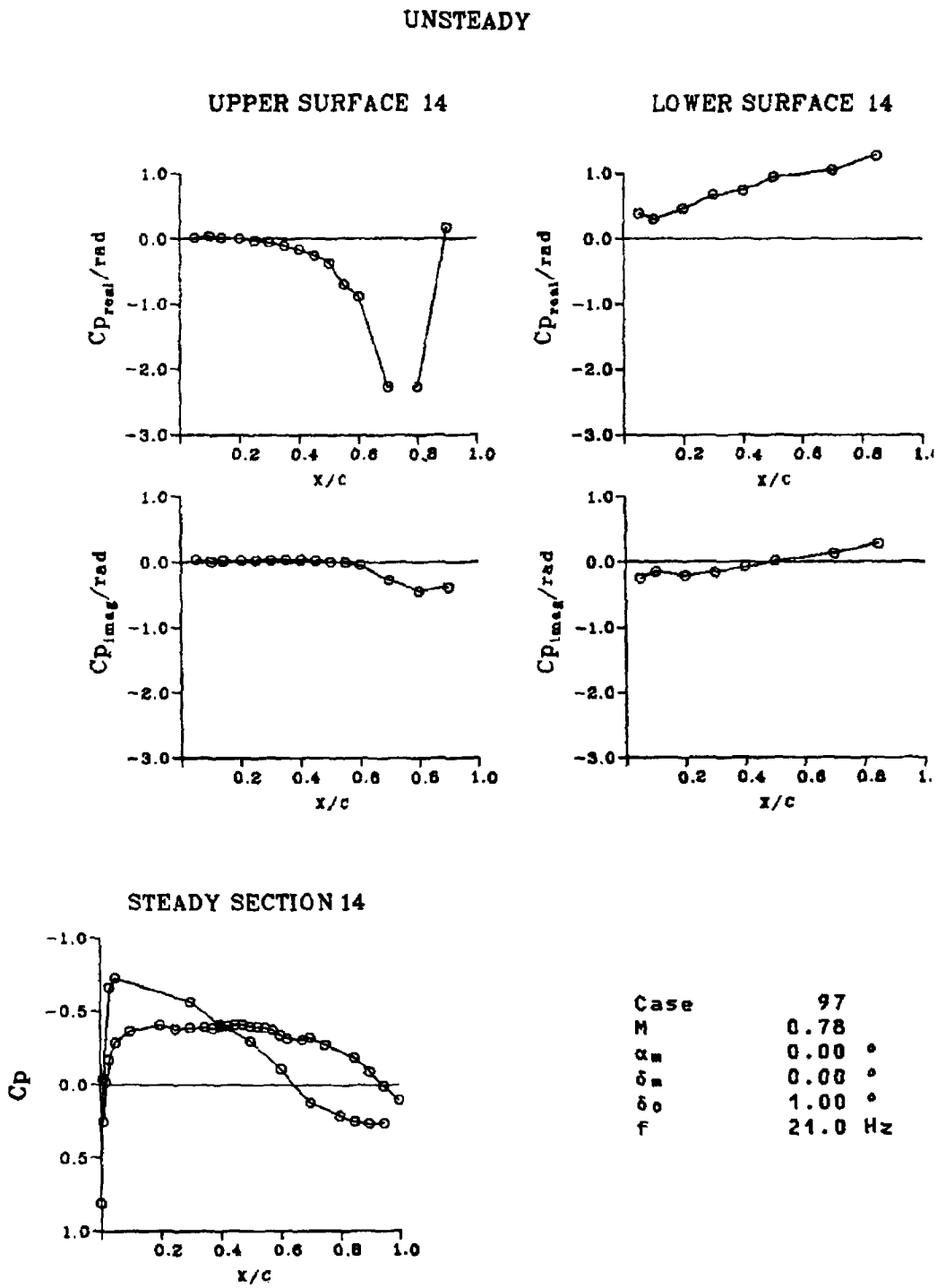

FIG. 9 Sample pressure distribution for aileron section

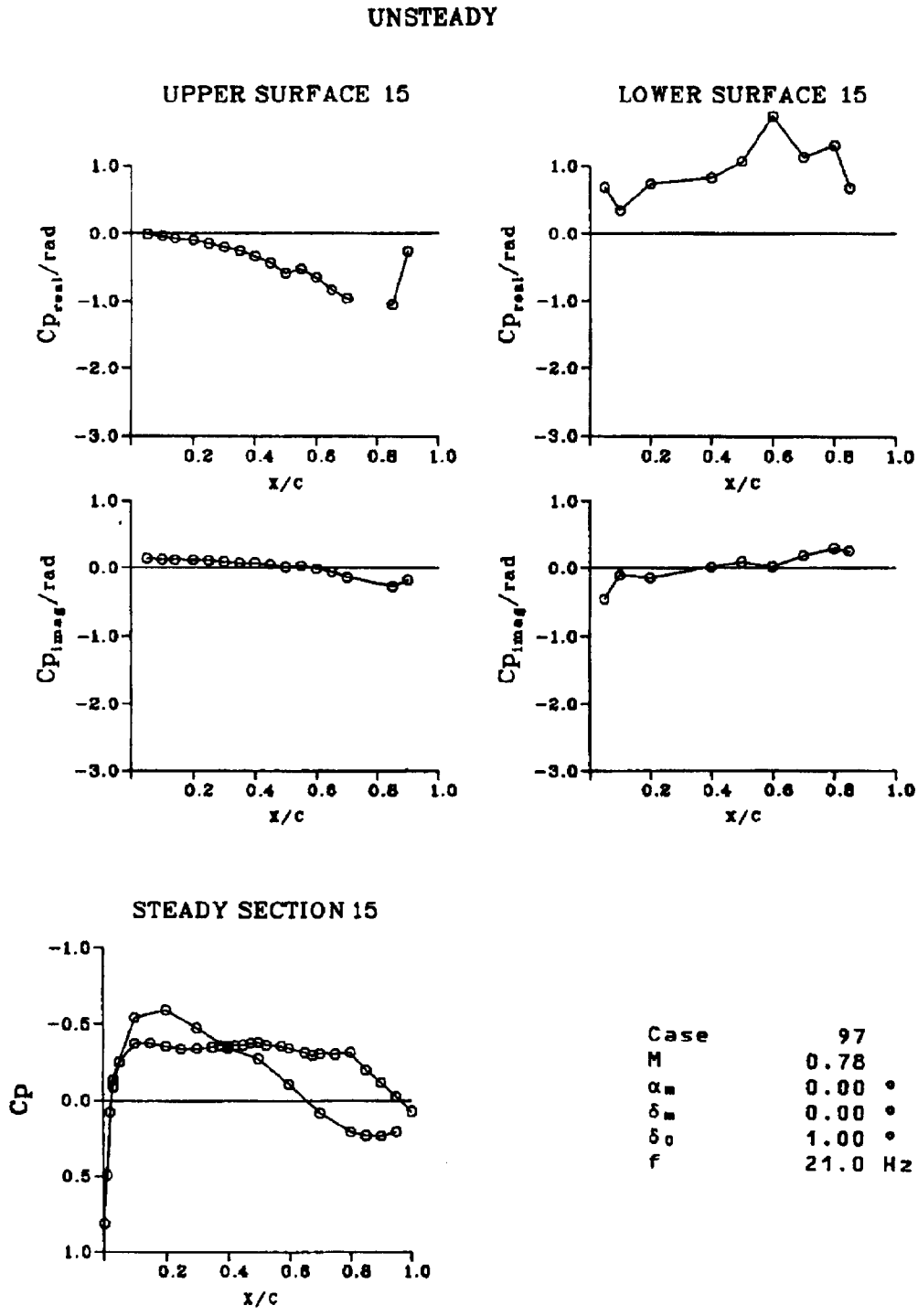

FIG. 10 Sample pressure distribution for aileron section

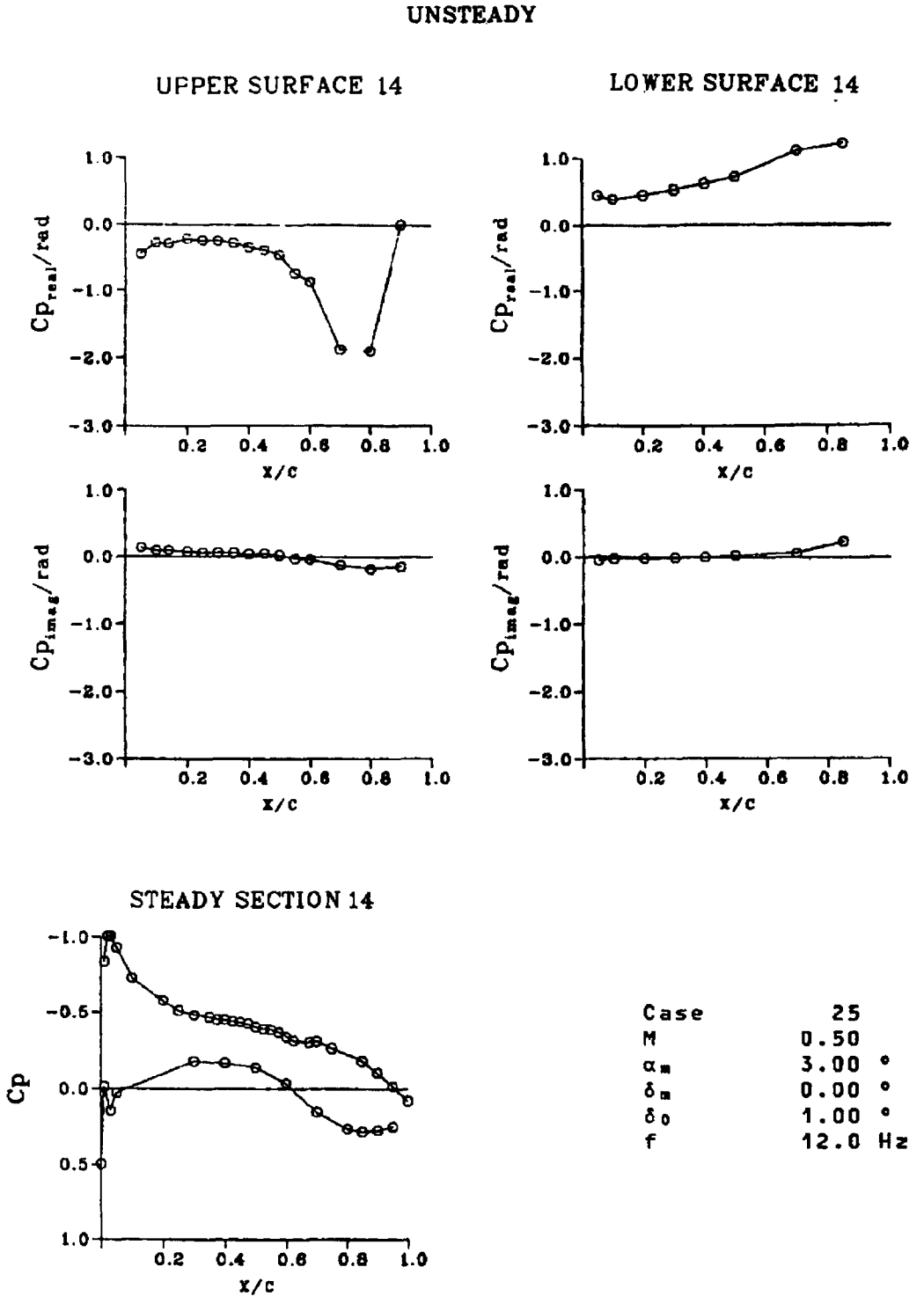

FIG. 11 Sample pressure distribution for aileron section

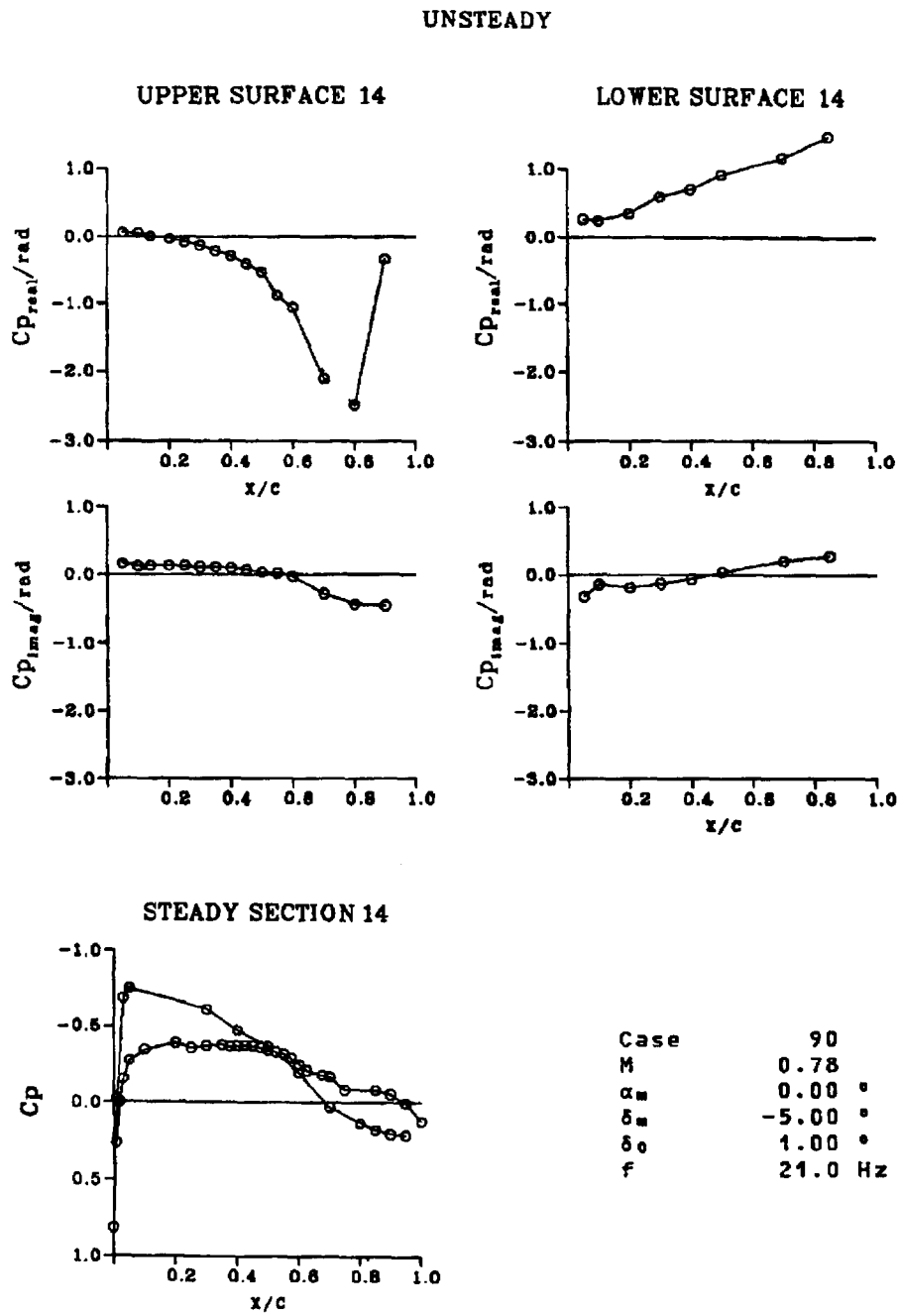

FIG. 12 Sample pressure distribution for aileron section

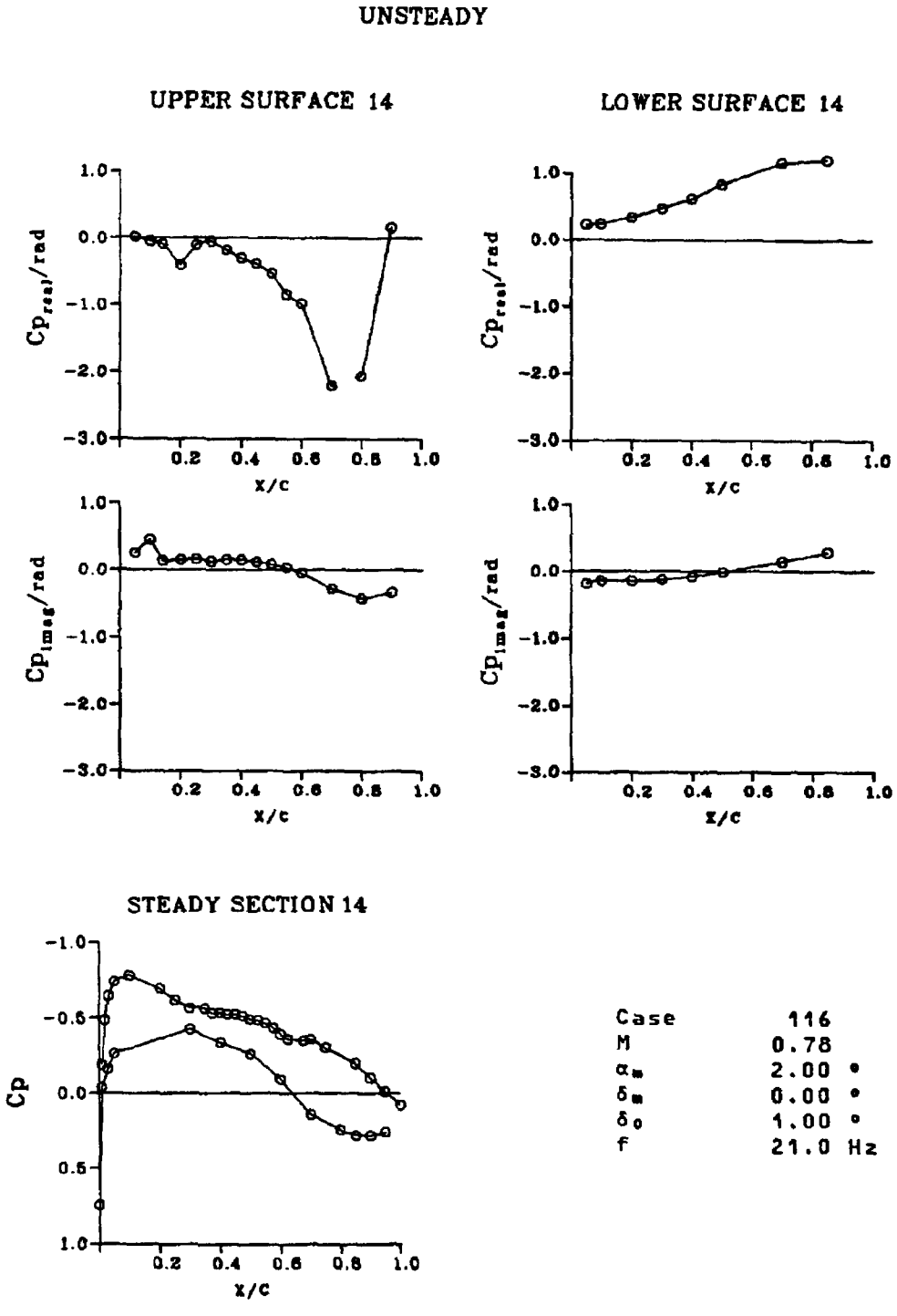

FIG. 13 Sample pressure distribution for aileron section

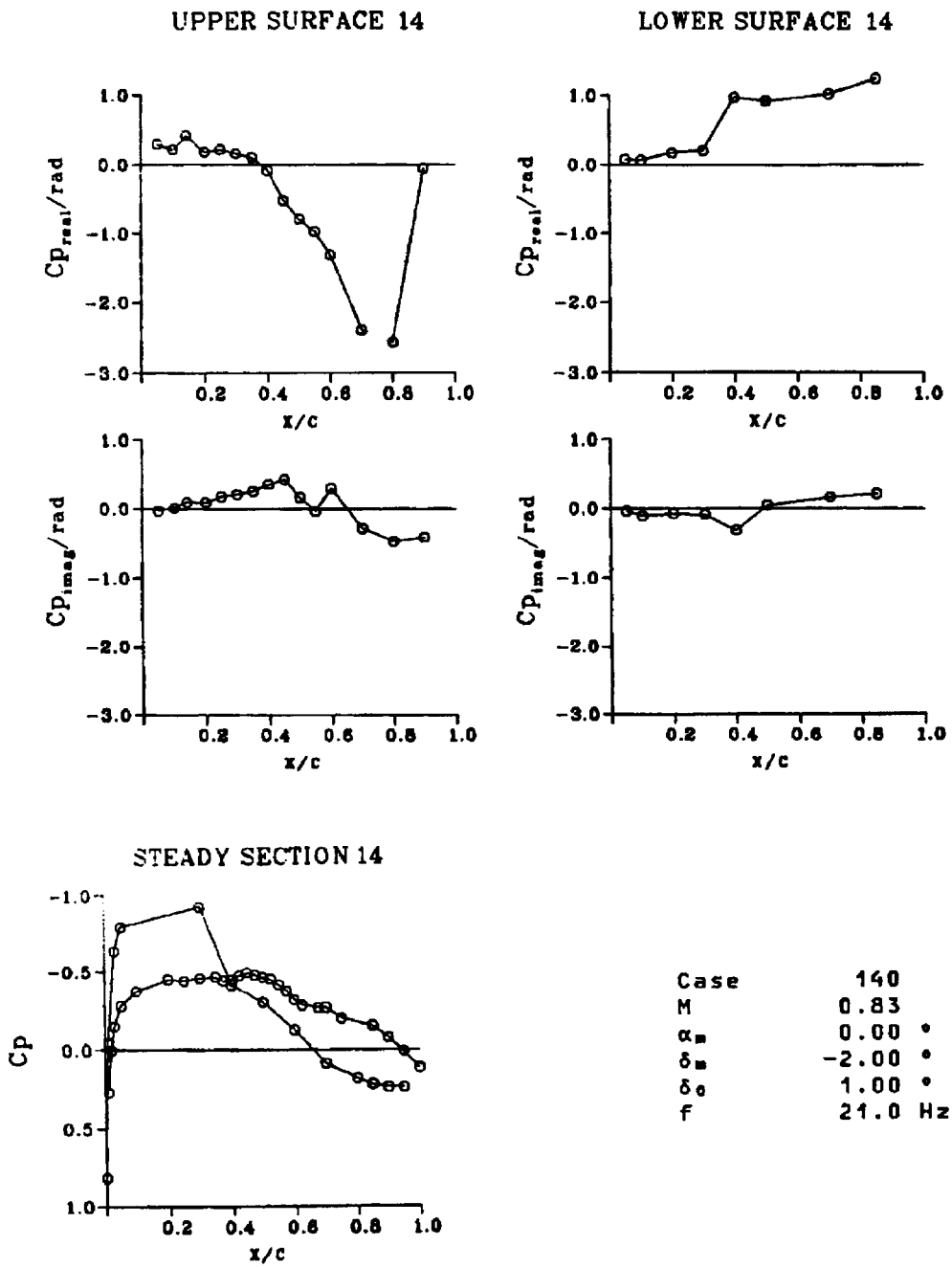

FIG. 14 Sample pressure distribution for aileron section

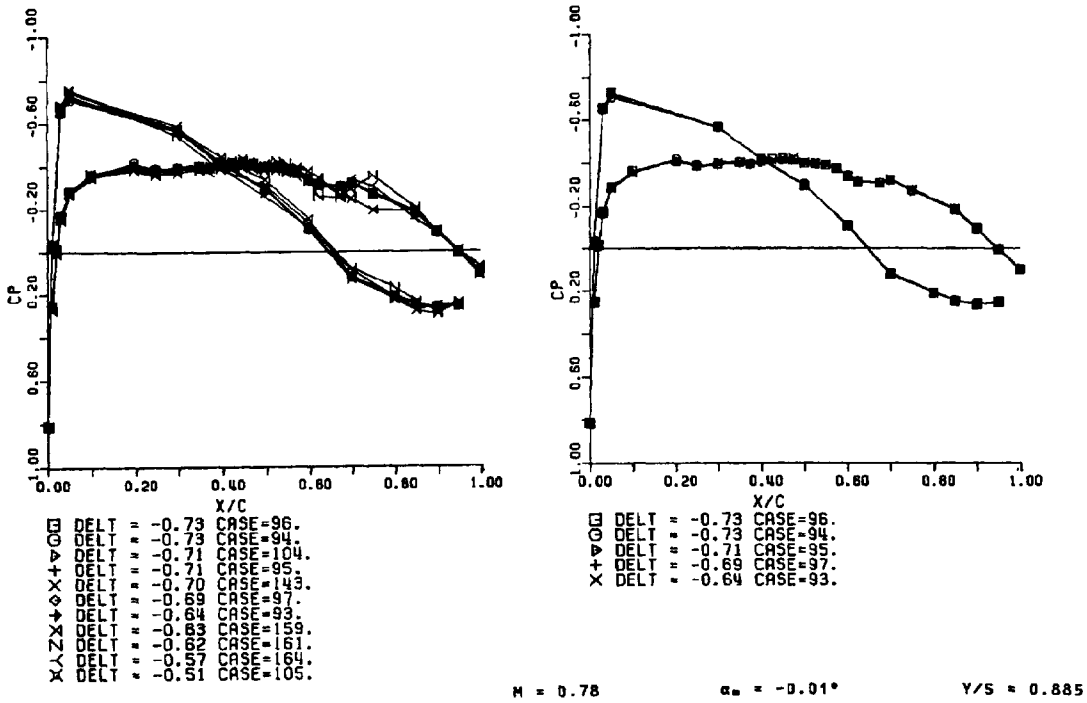

FIG. 15 Repeatability check for various cases